Introduction on van der Waals layered materials

Reza Asgari

IPM
Institute for Research in Fundamental Sciences

Workshop on Electronic properties of monolayer MoS2, October 2 (2013) IPM

van der Waals hetrostructures

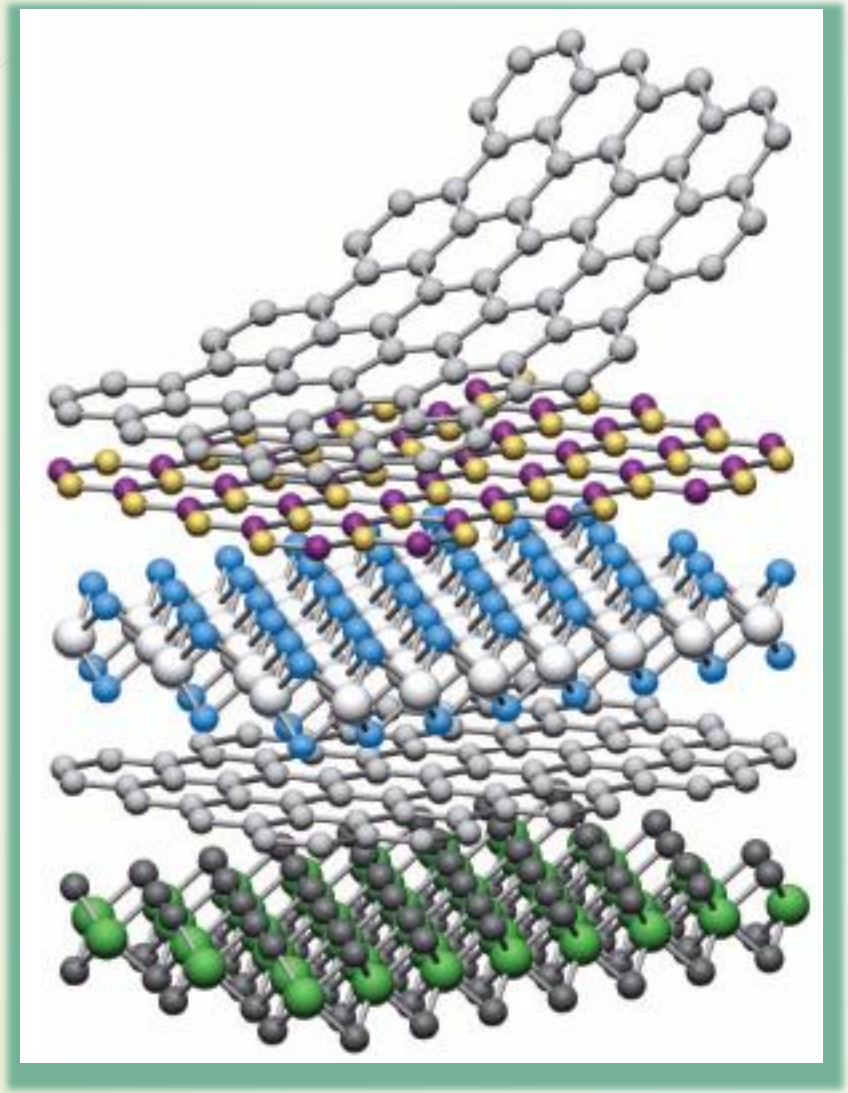

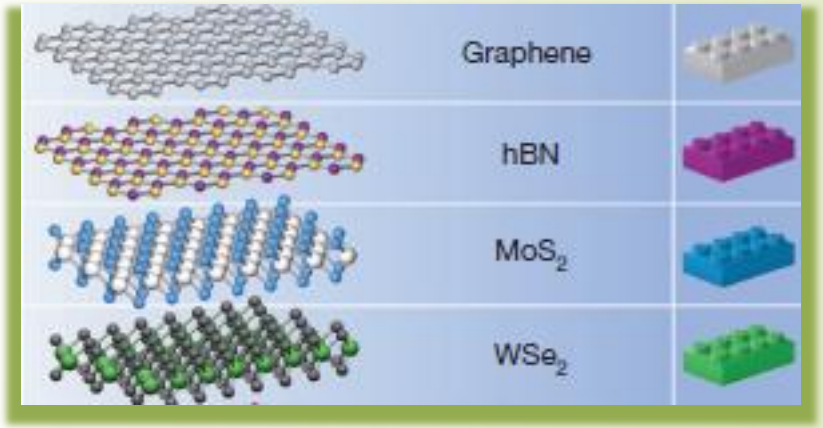

A. K. Geim and I . V. Grigoieva, Nature, **499**, 419 (2013)

Outline

- Introduction
- Graphene-like materials (BN, Silicene,..)
- TMDs, MoS2
- Conclusion

Layered van der Waals solids

These crystal structures feature neutral, single-atom-thick or polyhedral-thick layers of atoms that are covalently or ionically connected with their neighbors within each layer, whereas the layers are held together via van der Waals bonding along the third axis.

Layered van der Waals solids

- Mechanical exfoliation of large crystals using “Scotch tape”
- Chemical exfoliation

Novoselov, *et al* Nature **438**,197 (2005)

Epitaxy, requires ultrahigh vacuum conditions: Expensive Science **312**, 1192 (2006)
Various chemical methods. Nano Lett. **8,** 2442 (2008) , Nature Nanotech. 3, 270 (2008); *ibid* 4,217(2009)
Chemical Vapour Deposition : Nature **457**, 706 (2009), Nano Lett. **9**, 30 (2009)

Prerequisite for having 2D

- 3D materials with melting temperature over 1000
- 3D parents must be chemically inert and exhibit no decomposed surface layer in air
- Insulating and semiconducting 2D crystals are more likely to be stable than metallic ones

A. K. Geim and I . V. Grigoieva, Nature, **499**, 419 (2013)

Graphene

Many extraordinary properties, such as its 2.3% absorption in the white light spectrum, high Young's modulus and excellent thermal conductivity, have all been reported.

Using graphene in a wide range of areas, including high-speed electronic and optical devices, energy generation and storage, hybrid materials, chemical sensors, optoelectronics and even DNA sequencing.

M. Xu, T. Liang, M. Shi and H. Chen, Chemical Rev. **113**, 3766 (2013)

Different techniques:

Mechanical exfoliation, liquid-phase exfoliation, reduction of graphene oxide, chemical vapor deposition (CVD), surface segregation, and molecular beam epitaxy (MBE).

The fine control of the number and structure of graphene sheets over an entire substrate remains a major challenge.

Atomic structure: Graphene

- There are four valence electrons.
- The 2s and 2p can form hybridized orbital
- Two side-to-side $2p_z$ orbitals form a p bond
- Two co-axial $2p$ or sp orbitals form the s bond

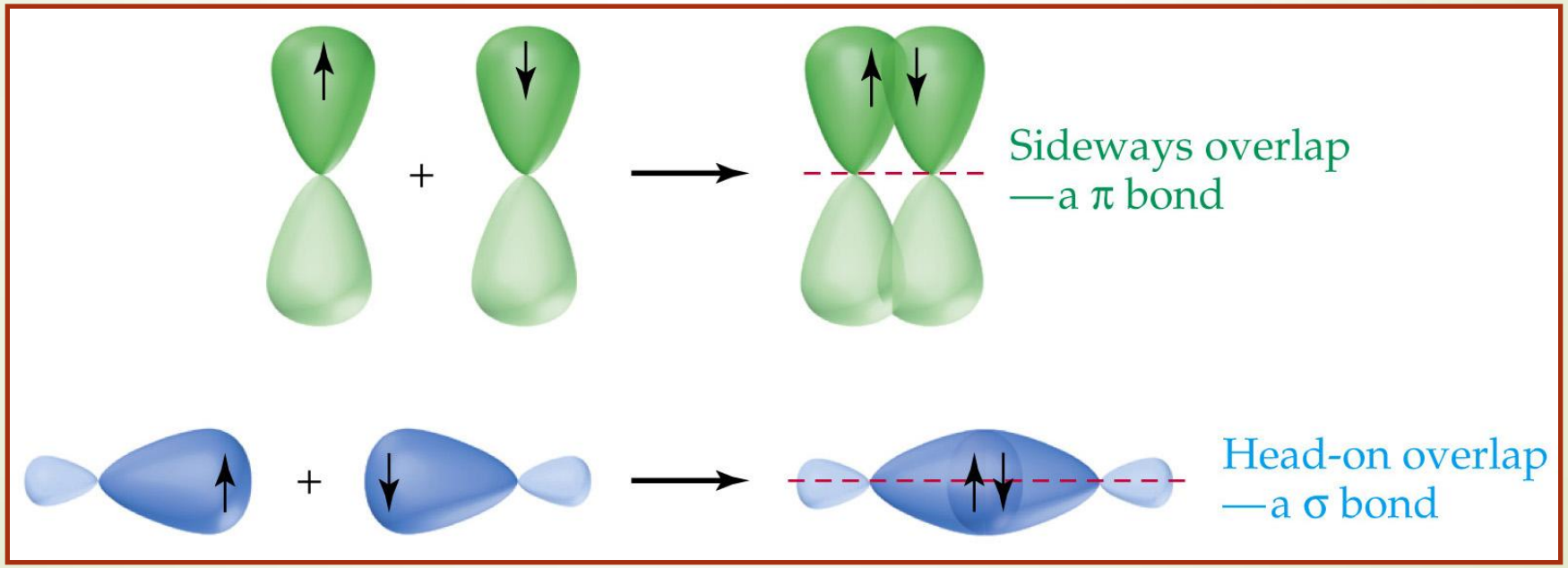

2D layered materials

metal chalcogenides, transition metal oxides, and other 2D compounds layered transition oxides such as MoO_3 and La_2CuO_4,22 insulator hexagonal boron nitride (h-BN), and topological insulators of Bi_2Te_3, Sb_2Se_3, Bi_2Se_3 and silicene and germanene

The common feature of these layered materials is that the bulk 3D crystals are stacked structures.

They involve van der Waals interactions between adjacent sheets with strong covalent bonding within each sheet.

2D layered materials: Library

<table>
<tr><td rowspan="1">Graphene family</td><td>Graphene</td><td colspan="2">hBN
‘white graphene’</td><td>BCN</td><td>Fluorographene</td><td>Graphene oxide</td></tr>
<tr><td rowspan="2">2D chalcogenides</td><td colspan="2" rowspan="2">MoS_2, WS_2, $MoSe_2$, WSe_2</td><td colspan="2" rowspan="2">Semiconducting dichalcogenides:
$MoTe_2$, WTe_2,
ZrS_2, $ZrSe_2$ and so on</td><td colspan="2">Metallic dichalcogenides:
$NbSe_2$, NbS_2, TaS_2, TiS_2, $NiSe_2$ and so on</td></tr>
<tr><td colspan="2">Layered semiconductors:
GaSe, GaTe, InSe, Bi_2Se_3 and so on</td></tr>
<tr><td rowspan="2">2D oxides</td><td>Micas,
BSCCO</td><td>MoO_3, WO_3</td><td rowspan="2" colspan="2">Perovskite-type:
$LaNb_2O_7$, $(Ca,Sr)_2Nb_3O_{10}$,
$Bi_4Ti_3O_{12}$, $Ca_2Ta_2TiO_{10}$ and so on</td><td>Hydroxides:
$Ni(OH)_2$, $Eu(OH)_2$ and so on</td></tr>
<tr><td>Layered
Cu oxides</td><td>TiO_2, MnO_2, V_2O_5,
TaO_3, RuO_2 and so on</td><td>Others</td></tr>
</table>

A. K. Geim and I . V. Grigoieva, Nature, **499**, 419 (2013)

Electronic band gaps

2D sheets	theoretical E_g (eV)	experimental E_g (eV)
graphene	0	0
bilayer graphene	0	0
bulk *h*-BN		5.97 [ref 52]
monolayer *h*-BN		6.07 [ref 65]
fully hydrogenized *h*-BN	3.05 [ref 66]	
2−5 layers *h*-BN		5.92 [ref 105.]
bulk MoS_2	1.20 (indirect[b]) [refs 35, 139]	1.0−1.29 (indirect) [refs 35, 139]
monolayer MoS_2[a]	~1.90 (direct[b]) [ref 140]	~1.90 (direct) [ref 140]
bulk WS_2	~1.30 (indirect[b]) [refs 35, 147]	~1.35 (indirect) [refs 35, 147]
monolayer WS_2[a]	~2.10 (direct[b]) [ref 147]	
	~1.80 (direct[c]) [ref 148]	
monolayer $MoSe_2$	~1.44 (direct[c]) [ref 148]	
monolayer $MoTe_2$	~1.07 (direct[c]) [ref 148]	

M. Xu, T. Liang, M. Shi and H. Chen, Chemical Rev. **113**, 3766 (2013)

Electronic structures:

From insulator to metal

lnclude the topological insulator effect, superconductivity, and thermoelectricity

Applications:

optoelectronics, spintronics, catalysts, chemical and biological sensors, supercapacitors, solar cells, and lithium ion batteries.

Specific examples

Boron Nitride

Hexagonal Boron Nitride

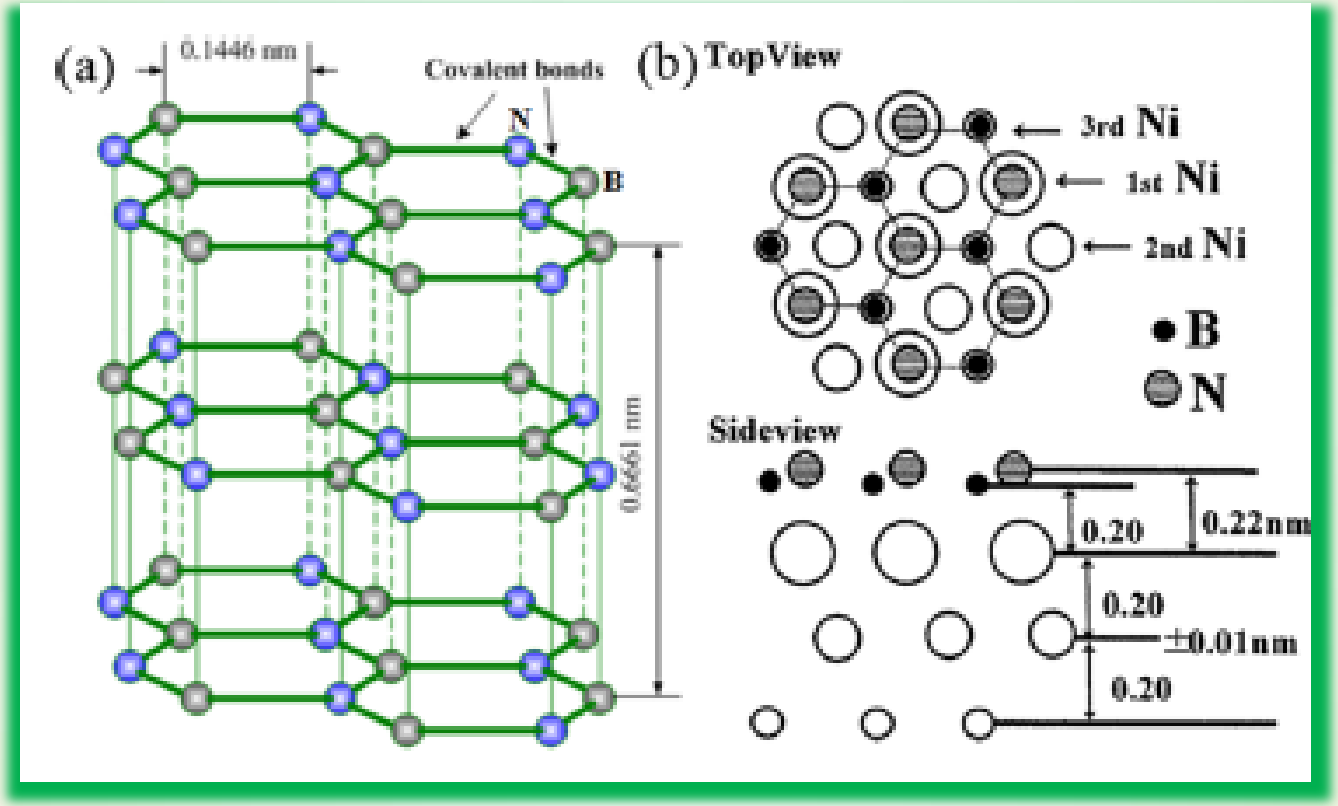

Bulk h-BN $E_g = 5.97\ eV$

monolayer h-BN $E_g = 6.07\ eV$

Topography and charge density

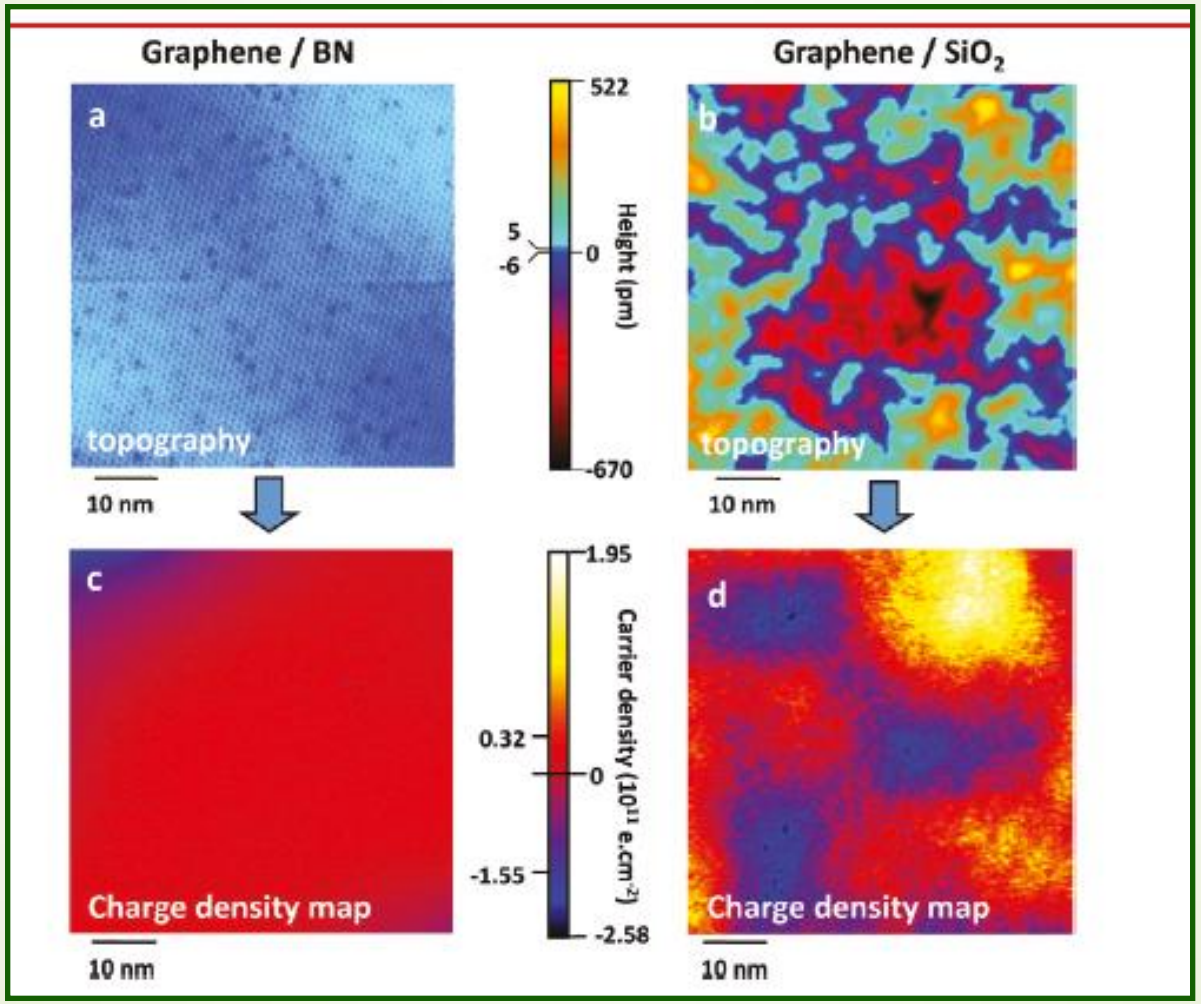

Decker, *et al*, Nano Letter, **11**, 2291 (2012)

Specific examples

Silicene

Silicene, Germanium and Tin

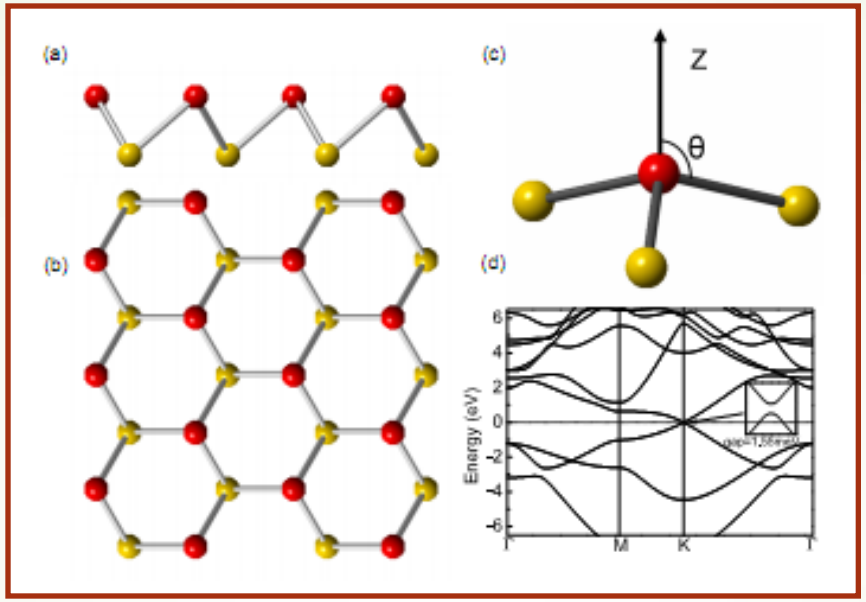

The lattice geometry of low-buckled silicene. Note that A sublattice (red) and B sublattice (yellow) are not coplanar. The angle is defined as being between the Si-Si bond and the z direction normal to the plane. Inset: zooming in the energy dispersion near the K point and the gap induced by SOC.

Silicene: Spin-orbit interaction

$$H_{so} = \frac{\hbar}{4m_0^2c^2}(\nabla V \times \vec{p}) \cdot \vec{\sigma} = -\frac{\hbar}{4m_0^2c^2}\left(\vec{F} \times \vec{p}\right) \cdot \vec{\sigma},$$

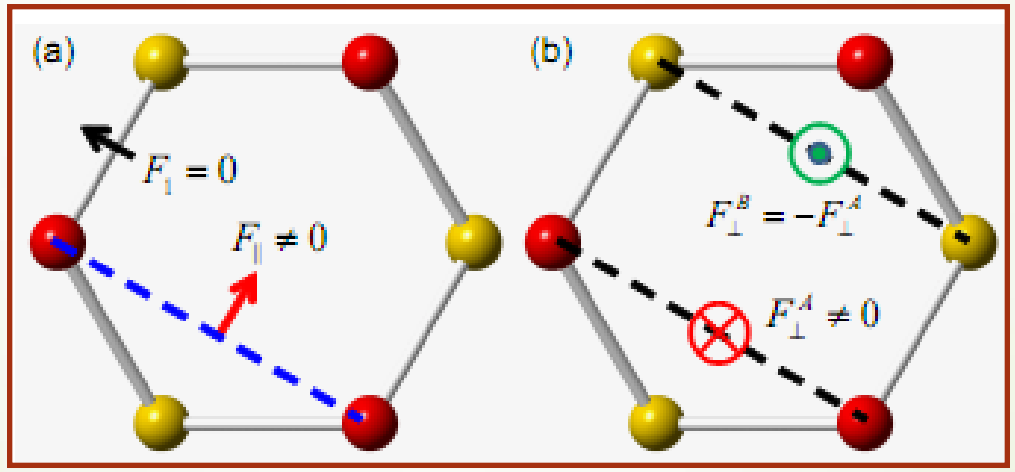

Cheng-Cheng Liu, Hua Jiang, and Yugui Yao, Phys. Rev. B (2011)

Low-energy model Hamiltonian

$$H_K^{eff}(\theta) = H_K \otimes I_2 + H_{so}^{1st} + H_{so}^{2st} + H_R(k)$$
$$= (\varepsilon_1 - \lambda_{so}^{2st}) I_4 + \begin{pmatrix} h_{11} & v_F k_+ \\ v_F k_- & -h_{11} \end{pmatrix},$$

$$h_{11} \equiv -\lambda_{so}\sigma_z - a\lambda_R(k_y\sigma_x - k_x\sigma_y)$$

$$k_+ = k_x + ik_y, k_- = k_x - ik_y,$$

$$\lambda_{so}^{2st} \equiv \left(\frac{\xi_0}{2}\right)^2 \frac{2}{9} \frac{-\Delta}{\sin^2\theta V_{sp\sigma}^2}.$$

$$v_F = \frac{-\sqrt{3}a}{2}[u_{11}^2(V_{pp\pi}\sin^2\theta + V_{pp\sigma}\cos^2\theta) - u_{21}^2 V_{ss\sigma}$$
$$+ 2u_{11}u_{21}\cos\theta V_{sp\sigma} - \tfrac{1}{2}|u_{31}|^2\sin^2\theta(V_{pp\sigma} - V_{pp\pi})],$$

$$\lambda_R = \frac{i\xi_0}{\sqrt{2}} \frac{u_{11}u_{32} - u_{31}u_{12}}{(\varepsilon_2 - \varepsilon_1)a} \times$$
$$[(u_{12}u_{21} + u_{22}u_{11})v_5 + u_{22}u_{21}v_7 + u_{12}u_{11}v_4 - 2u_{32}u_{31}v_1]$$
$$+ \frac{i\xi_0}{\sqrt{2}} \frac{u_{11}u_{33} - u_{31}u_{13}}{(\varepsilon_3 - \varepsilon_1)a} \times$$
$$[(u_{13}u_{21} + u_{23}u_{11})v_5 + u_{23}u_{21}v_7 + u_{13}u_{11}v_4 - 2u_{33}u_{31}v_1]$$
$$+ \xi_0 \frac{u_{11}\left(u_{11}v_3 - u_{21}v_6 - \frac{i}{\sqrt{2}}u_{31}v_2\right)}{2(V_1 + \varepsilon_1)a}$$
$$- \xi_0 \frac{u_{11}\left(-u_{11}v_3 + u_{21}v_6 - \frac{i}{\sqrt{2}}u_{31}v_2\right)}{2(V_1 - \varepsilon_1)a}.$$

$$\lambda_{so}^{1st} = \frac{\xi_0}{2}\frac{\varepsilon_1^2}{\alpha_1^2 V_3^2} \approx \frac{\xi_0}{2}\frac{2}{9}\frac{\Delta^2(V_{pp\pi} - V_{pp\sigma})^2}{V_{sp\sigma}^4}$$
$$\times \frac{\cot^2\theta}{1 + \frac{\cos^2\theta(V_{pp\pi} - V_{pp\sigma})^2}{V_{sp\sigma}^2}\left(1 + \frac{2}{9}\frac{\Delta^2}{\sin^2\theta V_{sp\sigma}^2}\right)}.$$

Silicene: Spin-orbit interaction

System	$a(\text{Å})$	θ	$\lambda_{so}^{1st}\,(meV)$	λ_{so}^{2st}	λ_R	$Gap\,(meV)\,(TB)$	$Gap(FP)$	$v_F\,(10^5 m/s)\,(TB)$	$v_F(FP)$
graphene	2.46	90°	0	1.3×10^{-3}	0	2.6×10^{-3}	0.8×10^{-3}[a]	9.80	8.46
silicene	3.86	101.7°	3.9	7.3×10^{-2}	0.7	7.9	1.55[b]	5.52	5.42
ge(licene)	4.02	106.5°	43	3.3	10.7	93	23.9[b]	4.57	5.24
sn(licene)	4.70	107.1°	29.9	34.5	9.5	129	73.5	4.85	4.70

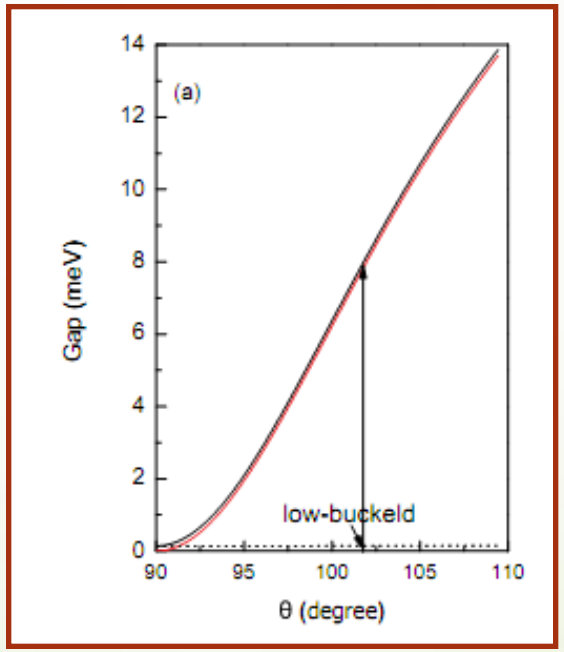

Evidence for Dirac fermions: Silicene

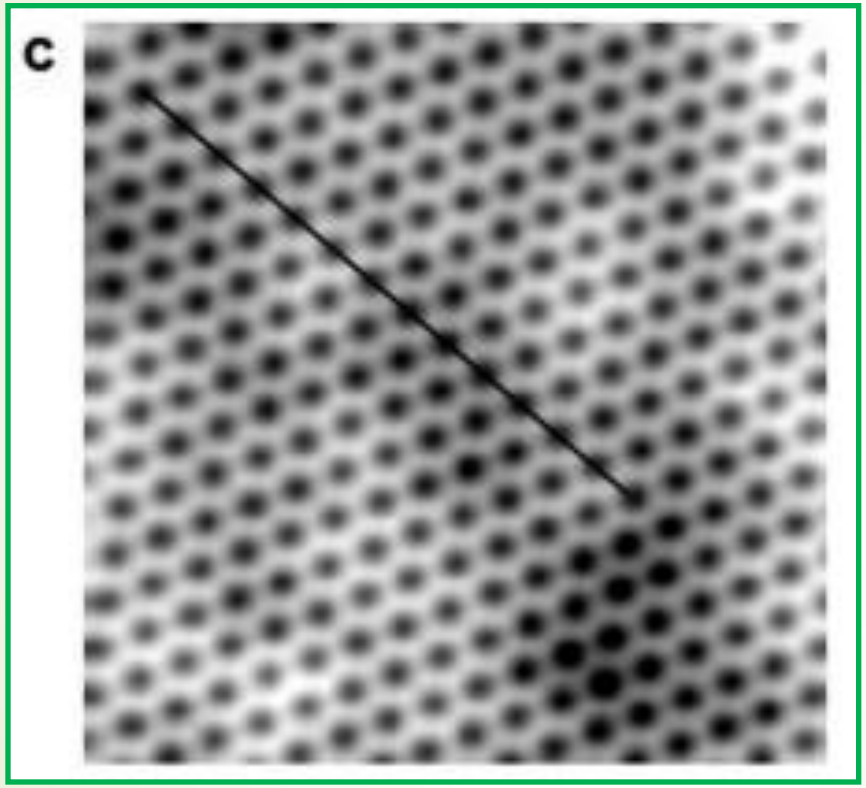

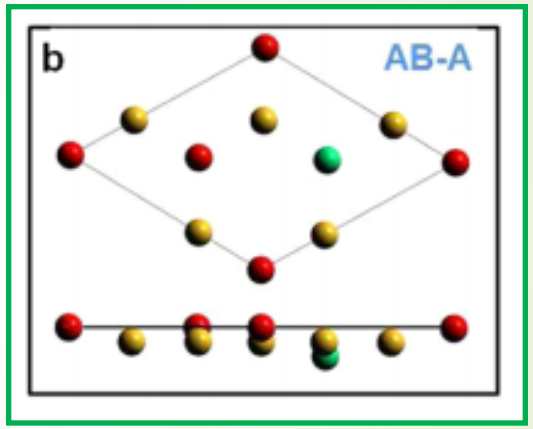

L. Chen, et al Phys. Rev. Lett. **109**, 056804 (2012)

Silicene: Topological phase transition

$$H_0 = -t \sum_{\langle i,j \rangle \alpha} c^\dagger_{i\alpha} c_{j\alpha} + i\frac{\lambda_{\rm SO}}{3\sqrt{3}} \sum_{\langle\langle i,j \rangle\rangle \alpha\beta} \nu_{ij} c^\dagger_{i\alpha} \sigma^z_{\alpha\beta} c_{j\beta} - i\frac{2}{3}\lambda_{\rm R2} \sum_{\langle\langle i,j \rangle\rangle \alpha\beta} \mu_i c^\dagger_{i\alpha} \left(\boldsymbol{\sigma} \times \hat{\boldsymbol{d}}_{ij}\right)^z_{\alpha\beta} c_{j\beta},$$

νij= +1 if the second-nearest-neighboring hopping is anticlockwise and -1 if it is clockwise with respect to the positive z axis. The third term represents the Rashba SO coupling with λR = 0.7meV, where μi = ±1 for the A (B) site, and dij= dij/ |dij| with dij the vector connecting two sites i and j in the same sublattice.

$\ell = 0.23$Å

$$H_E = i\lambda_{\rm R1}(E_z) \sum_{\langle i,j \rangle \alpha\beta} c^\dagger_{i\alpha} \left(\boldsymbol{\sigma} \times \hat{\boldsymbol{d}}_{ij}\right)^z_{\alpha\beta} c_{j\beta} + \ell \sum_{i\alpha} \mu_i E^i_z c^\dagger_{i\alpha} c_{i\alpha},$$

$\lambda_{\rm R1}(E_z) \propto E_z$

10μeV at $E_z = \lambda_{\rm SO}/\ell = 17$meVÅ^{-1}

M. Ezawa, Eur. Phys. J. B **85**, 363 (2012)

Silicene: Topological phase transition

$$\Delta_s(E_z) = -s\lambda_{SO} + \frac{1}{2}\ell E_z + \frac{1}{2}\sqrt{(\ell E_z)^2 + \lambda_{R1}^2}.$$

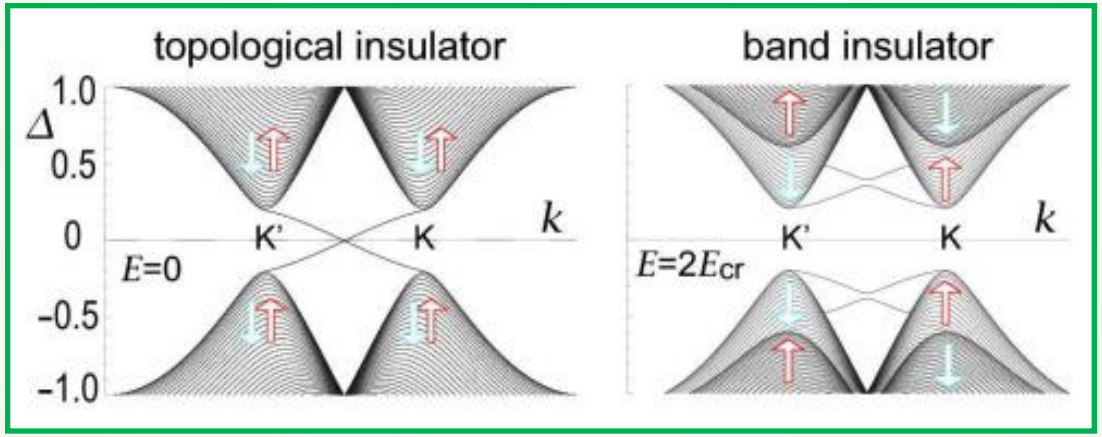

$$E_{cr} = \frac{s\lambda_{SO}}{\ell}\left[1 - \left(\frac{\lambda_{R1}}{2\lambda_{SO}}\right)^2\right] = \pm 17\text{meV/Å},$$

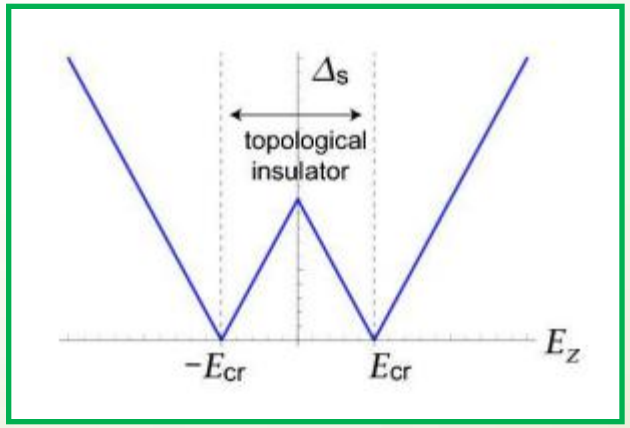

Specific examples

Transition metal dichalcogenides

Transition metal dichalcogenides

From insulator to superconductor

Include the semiconductivity, half-metallic magnetism, superconductivity, or charge density wave

Applications:

lubrication, catalysis, photovoltaics, supercapacitors, and rechargeable battery systems.

Examples: Layered van der Waals solids

- Graphene
- Silicene, Germanium, Tin
- Transition metal dichalcogenid materials , MX_2 (M = Ti, Zr, Hf, V, Nb, Ta, Re; X = S, Se, Te)

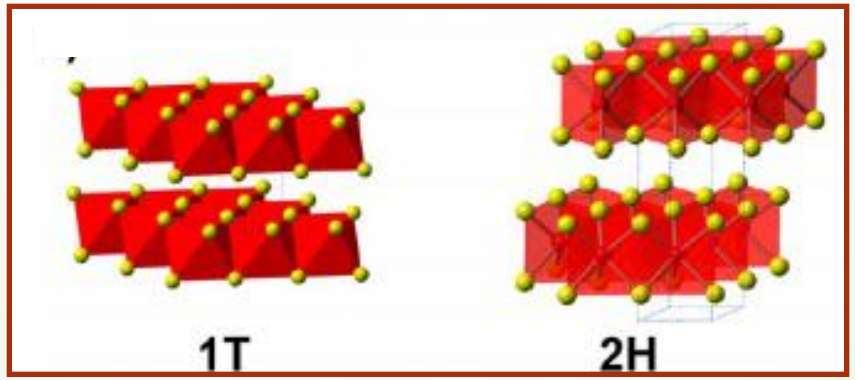

Mattheis, Phys. Rev. B **8**, 3719 (1973)
Helveg, et al Phys. Rev. Lett. **84**, 951 (2000)

Wang, Kalantar Zadeh, Kis, Coleman, Strano, Nature Nanotech. **7**, 699 (2012)

Examples: Layered van der Waals solids

Many novel van der Waals compounds can be created via precursor solids.

For example, the layered CaGe can be layerd in aqueous HCl to produce monolayer

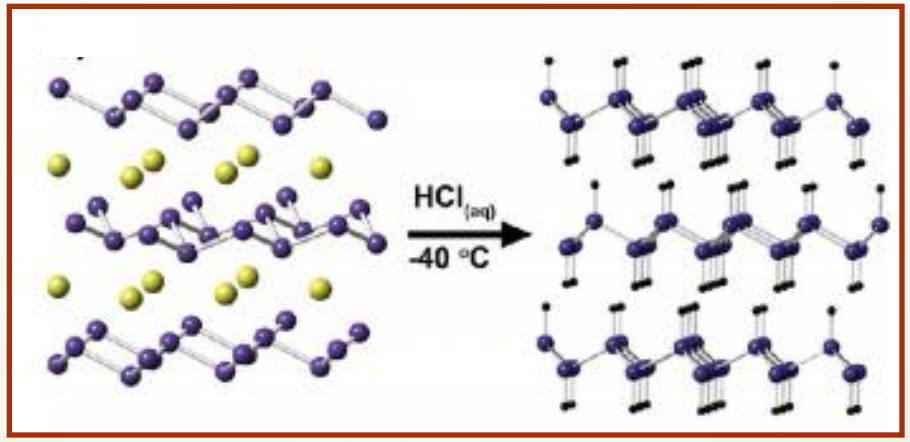

Bianco, E.; Butler, S.; Jiang, S.; Restrepo, O. D.; Windl, W.;Goldberger, J. E. ACS Nano 2013
Vogg, G.; Brandt, M. S.; Stutzmann, M. Polygermyne Adv. Material. 12, 1278 (2000)

TMDCs: MoS2 crystal

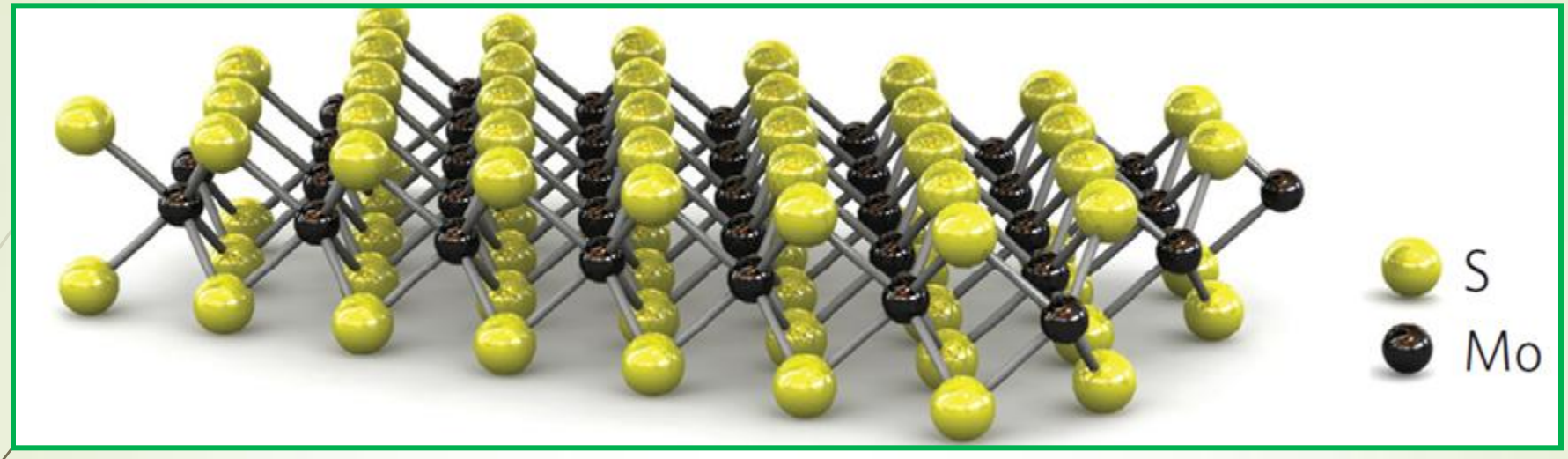

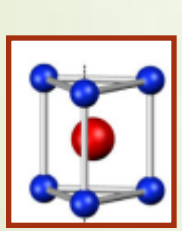

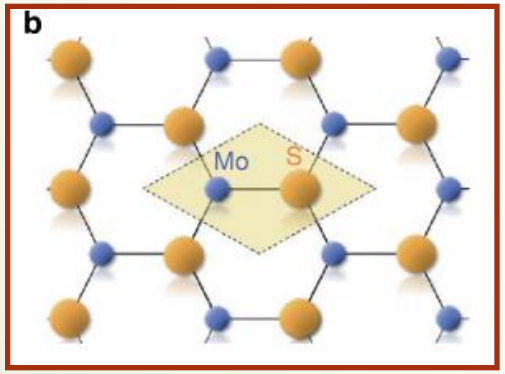

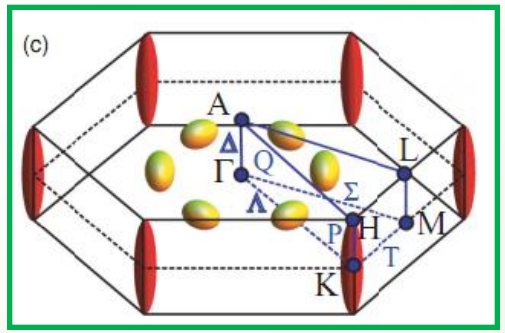

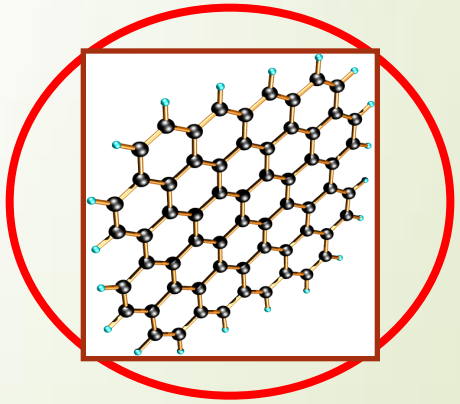

Wilson and Yaffe, Adv. Phys. **18**, 193 (1969)
Romley, Murray,Yoffe, J. Phys. C **5** (1972)
Mattheis, Phys. Rev. B **8**, 3719 (1973)
Helveg, *et al.*, Phys. Rev. Lett. **84**, 951 (2000)

kobayashi, Yamauchi, Phys. Rev. B **51**, 17085 (1995)

Transition metal dichalcogenides

2H-MX_2

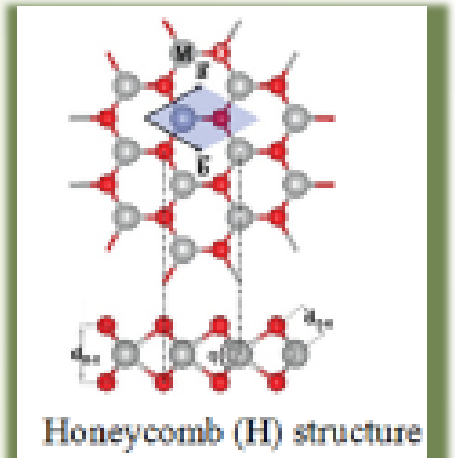

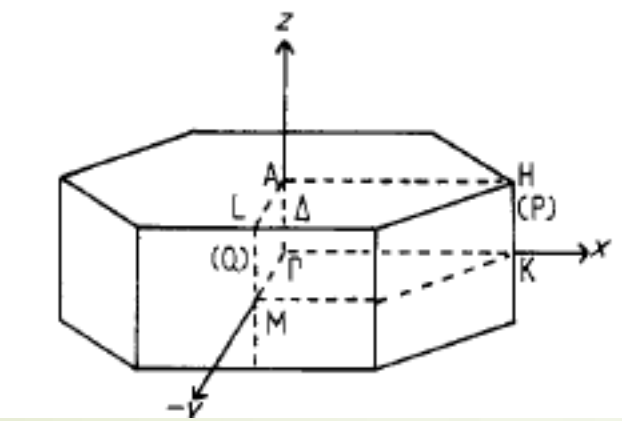

1T-MX_2

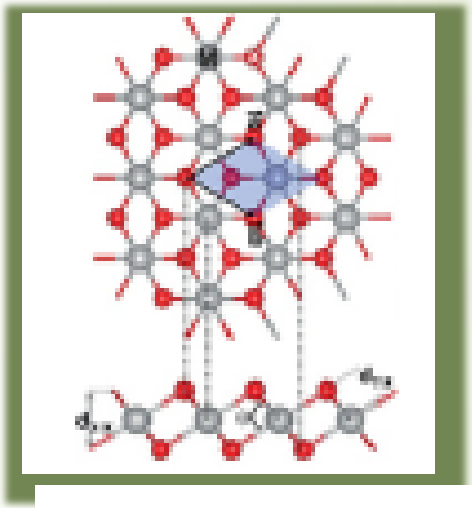

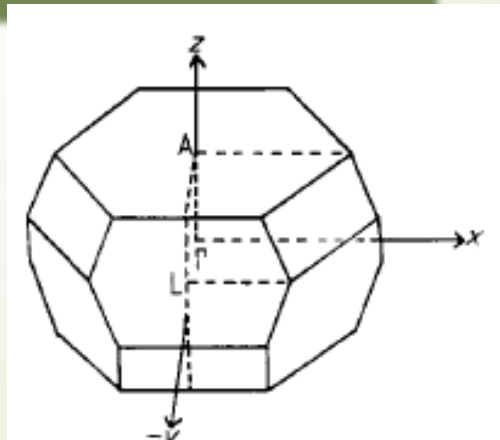

Transition metal dichalcogenides

	3d							4d	5d
H^{**}(1.05) ScO_2 T^{+}	TiO_2	VO_2 H^{*}	CrO_2 H^{**}(0.50)	H^{*} MnO_2 T^{**}(0.28)	FeO_2 H^{*}	CoO_2	NiO_2 T^{**}(1.38)	NbO_2	MoO_2 H^{**}(0.97)	WO_2 H^{**}(1.37)
H^{**}(0.44) ScS_2 T^{*}	TiS_2 T^{*}	T^{*} VS_2 H^{*}	CrS_2 H^{**}(1.07)	MnS_2 T^{*}	FeS_2 H^{*}	CoS_2	H^{*} NiS_2 T^{**}(0.51)	NbS_2 T^{*}	MoS_2 H^{**}(1.87)	WS_2 H^{**}(1.98)
H^{**}(0.27) $ScSe_2$ T^{*}	$TiSe_2$ T^{*}	H^{*} VSe_2 T^{*}	$CrSe_2$ H^{**}(0.86)	$MnSe_2$ T^{*}	$FeSe_2$ H^{*}	$CoSe_2$	H^{*} $NiSe_2$ T^{**}(0.10)	T^{*} $NbSe_2$ H^{*}	$MoSe_2$ H^{**}(1.62)	WSe_2 H^{**}(1.68)
H^{*} $ScTe_2$ T^{*}	H^{*} $TiTe_2$ T^{*}	H^{*} VTe_2 T^{*}	$CrTe_2$ H^{**}(0.60)	$MnTe_2$ T^{*}	$FeTe_2$ H^{*}	$CoTe_2$ H^{*}	H^{*} $NiTe_2$ T^{*}	$NbTe_2$ T^{*}	$MoTe_2$ H^{**}(1.25)	WTe_2 H^{**}(1.24)

H & T unstable | H stable | T stable | H & T Stable E_c[T]>E_c[H] | H & T Stable E_c[T]<E_c[H]

E_c: cohesive energy per MX_2 unit
T^{+}: half-metal; T^{*} & H^{*}: metal
T^{**} & H^{**}: semiconductor (E_g/eV)

direct band gap
indirect band gap

Band structures

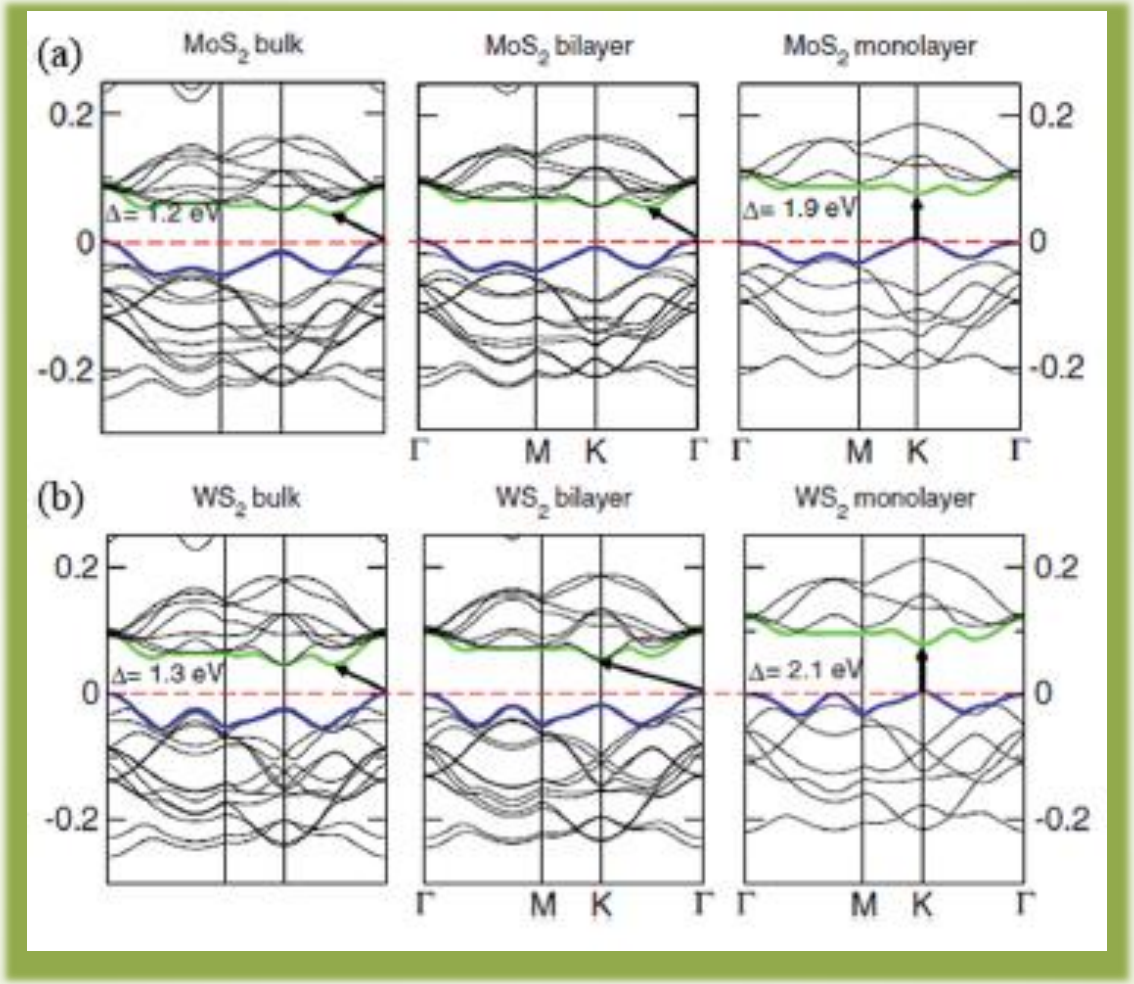

W. S. Yun, *et al*, Phys. Rev. B **85**, 033305 (2012)

ARPES measurements of the electronic structure

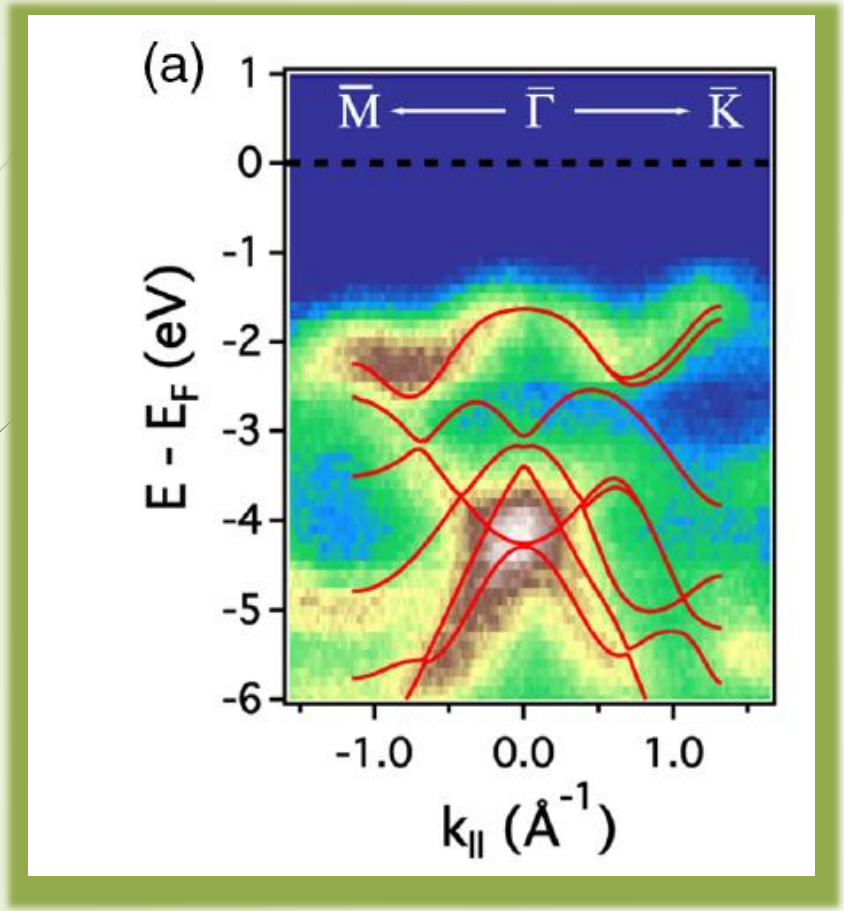

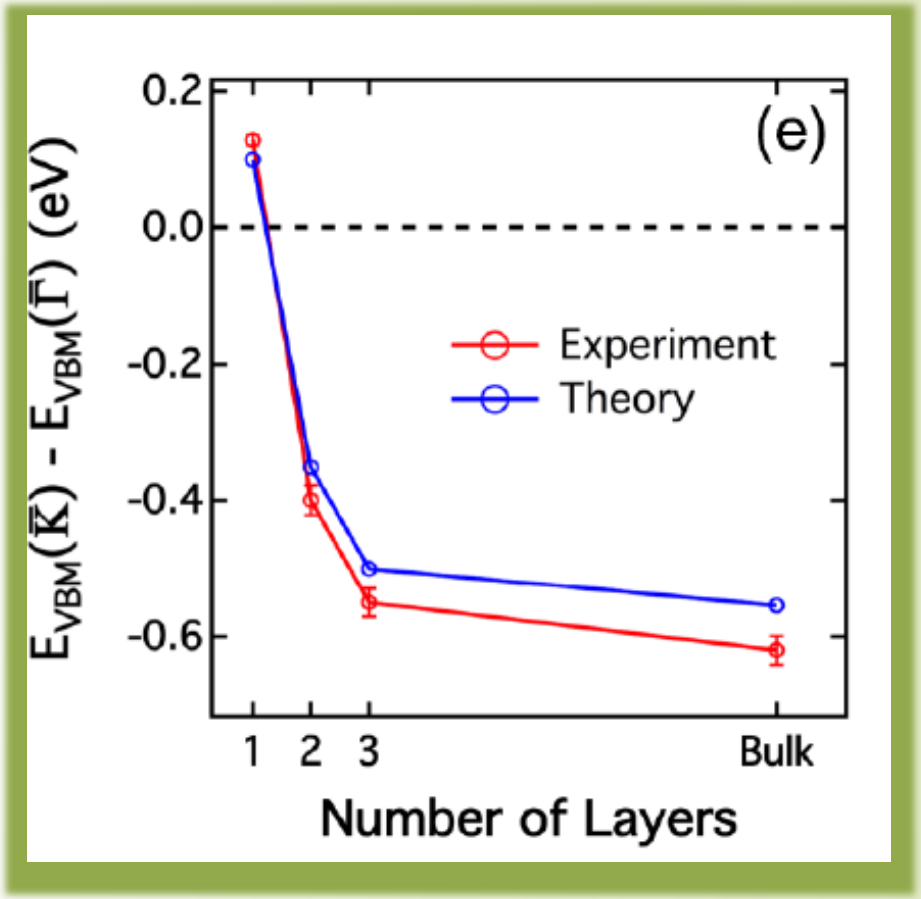

W. Jin, *et al*, Phys. Rev. Lett. **111**, 106801 (2013)
E. Cappelluti, *et al* Phys. Rev. B **88**, 075409 (2013).

Strain effects on the electronic properties of TMDs

Strain in a crystalline solid
modifies the lattice constants and reduces the
crystal symmetry, leading to significant shifts in the energy band edges

Strain effects on the electronic properties of TMDs

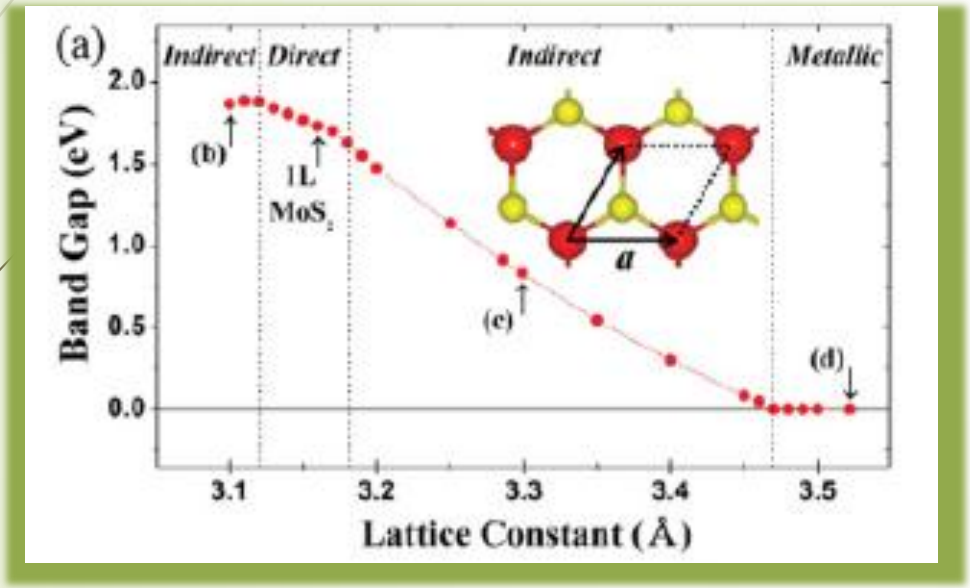

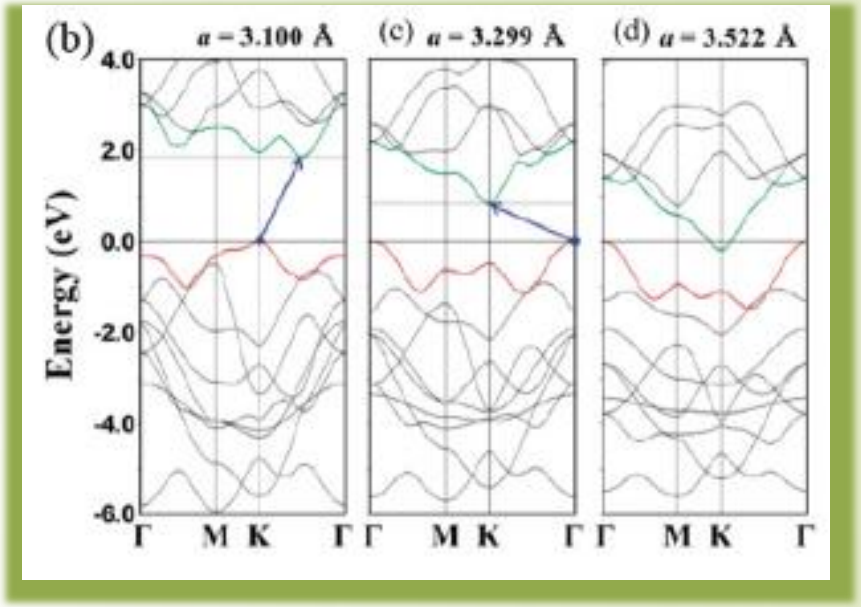

W. S. Yun, *et al*, Phys. Rev. B 85, 033305 (2012)

Electric field on Armchair MoS2

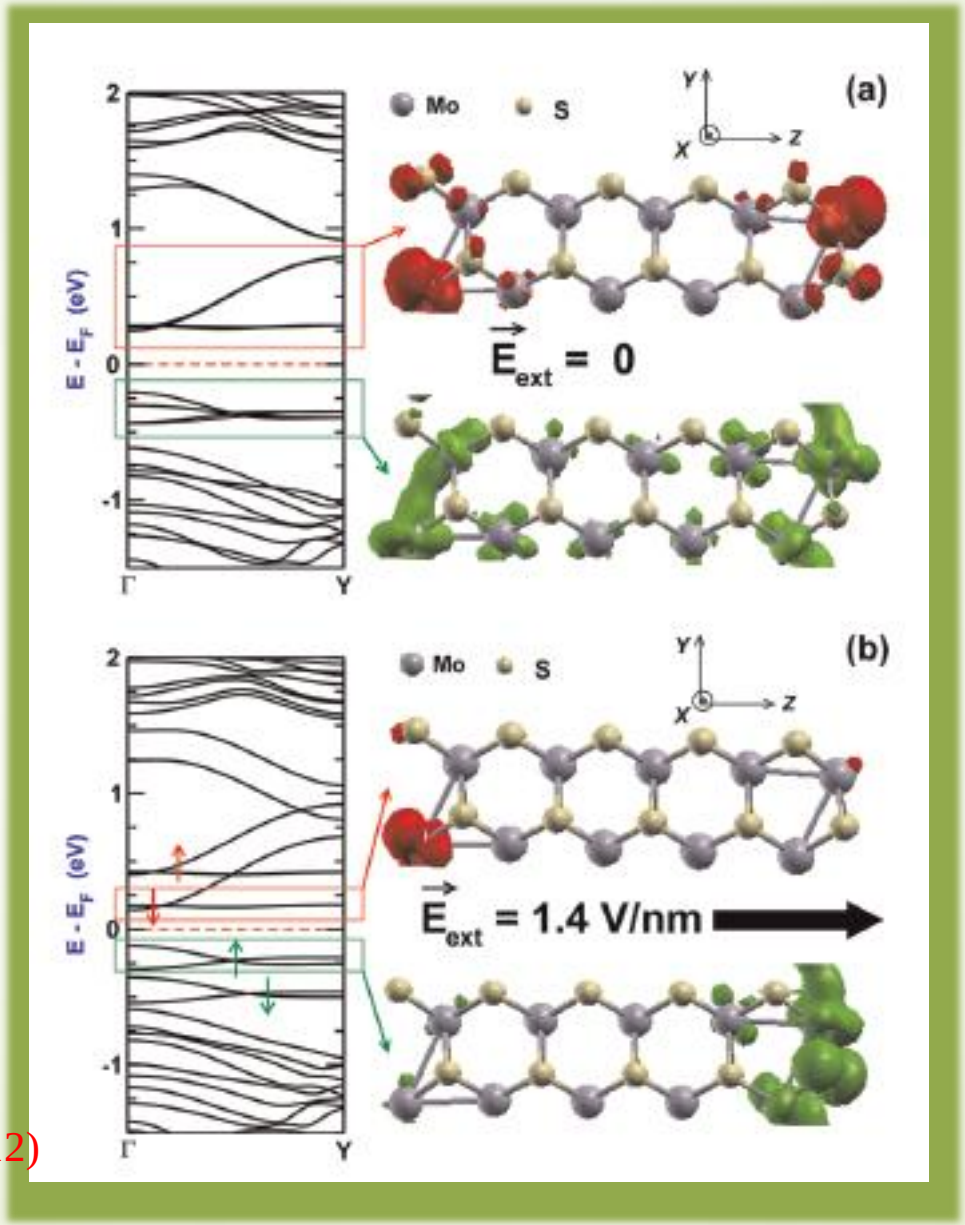

Dolui, *et al*, Acs Nano 6, 4823 (2012)

Band gap in the applied transverse electric field

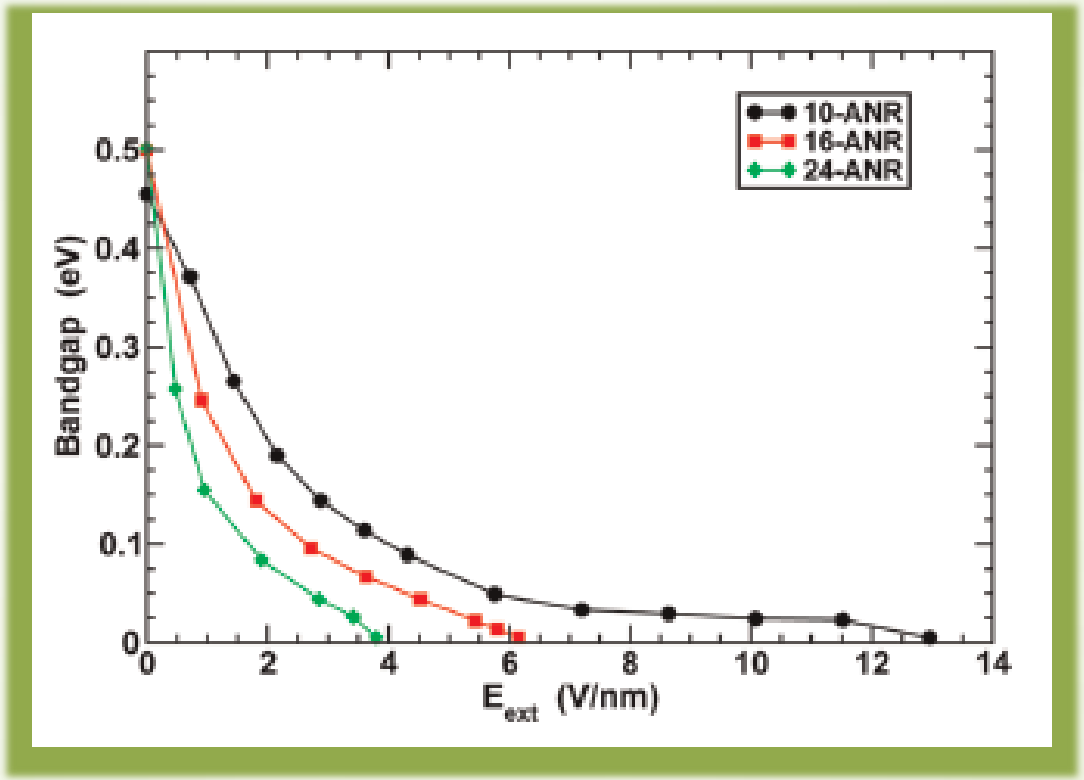

Dolui, *et al*, Acs Nano 6, 4823 (2012)

TMDCs: MoS2 crystal

Photoluminescence properties

[Kr] $5s^1\ 4s^2p^6d^5$
2 ,8 ,18 ,13 ,1

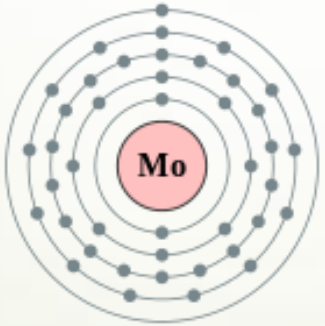

[Ne] $3s^2\ 3p^4$
2 ,8 ,6

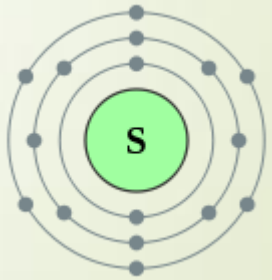

Wang, Kalantar Zadeh, Kis, Coleman, Strano, Nature Nanotech. **7**, 699 (2012)

Spectroscopy: few layers

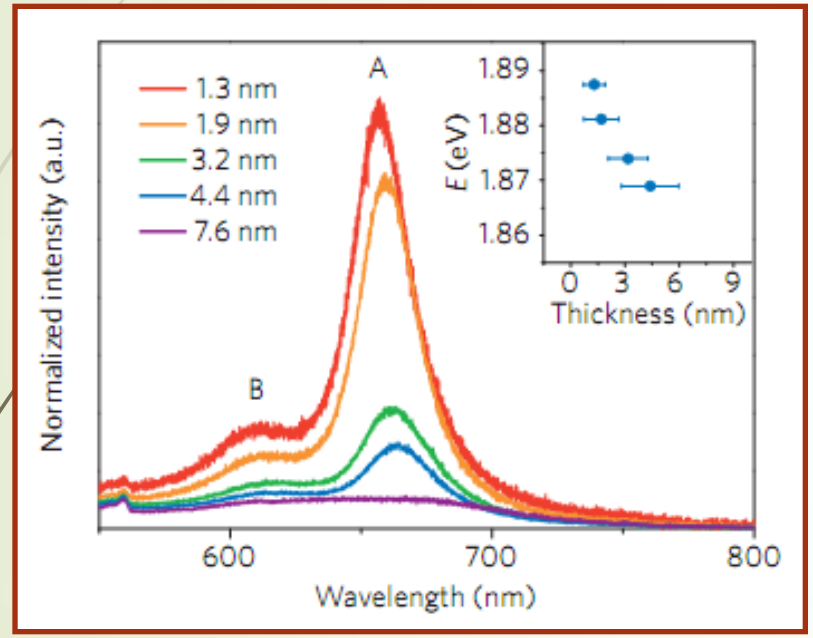

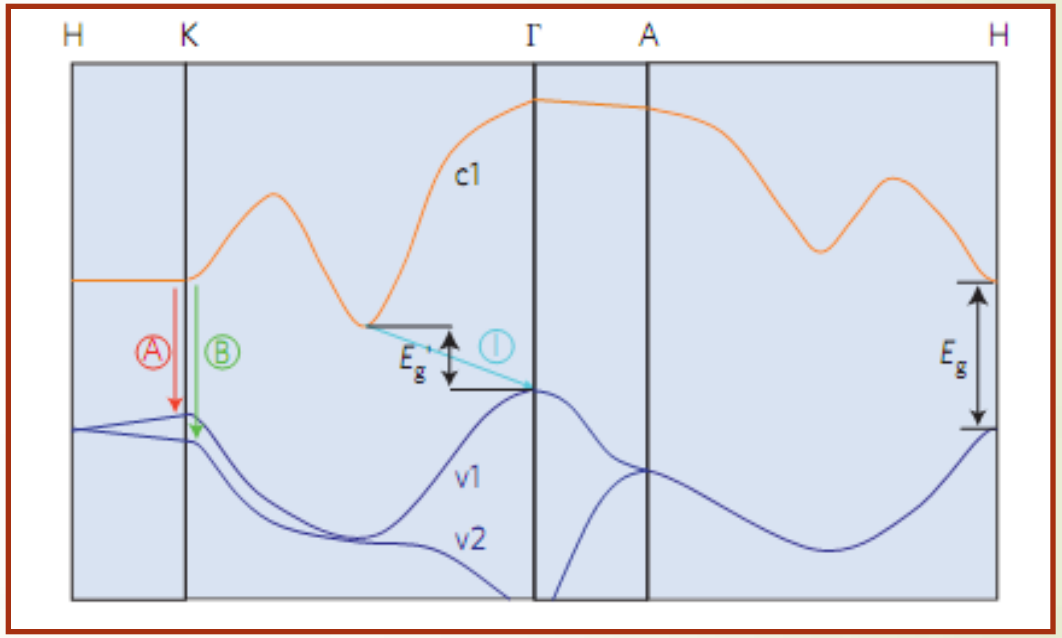

Eda, *et al*, Nano Lett. **11**, 5111 (2011)

Mak *et al*, Phys. Rev. Lett. **105**, 136805 (2010)

Valley polarization

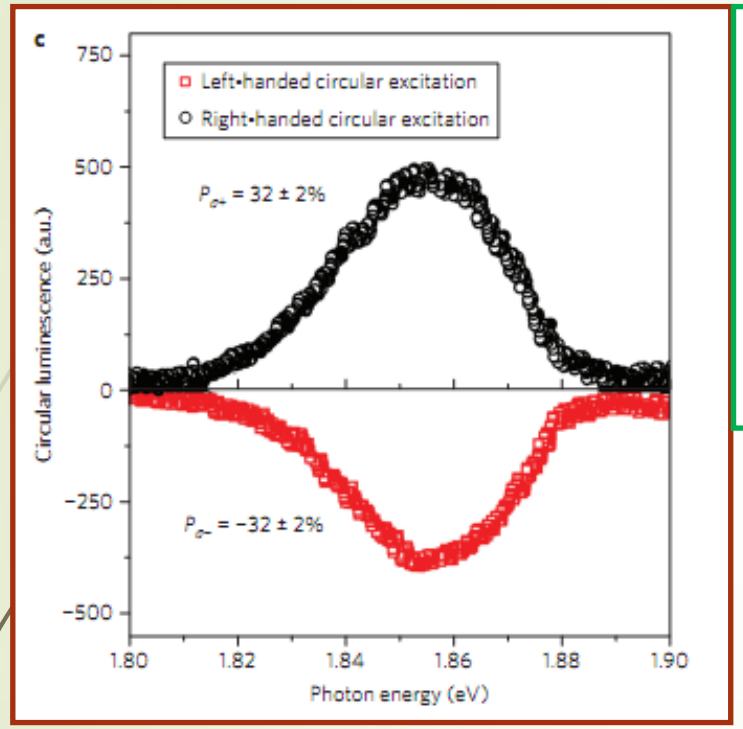

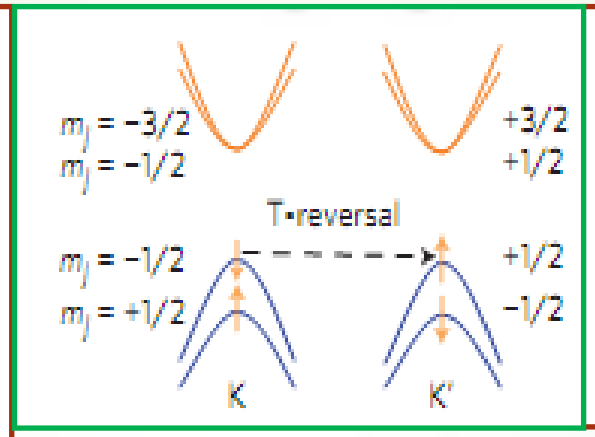

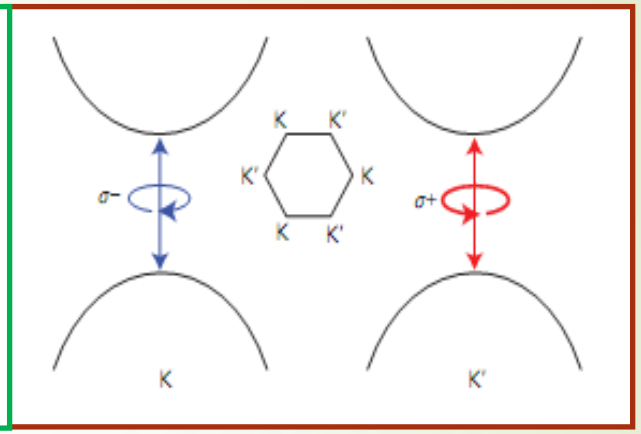

$$\Delta m = \pm 1$$

$$P = \frac{|P_+^{vc}|^2 - |P_-^{vc}|^2}{|P_+^{vc}|^2 + |P_-^{vc}|^2}$$

$$P_\pm^{vc}(k) = \langle u_c(k) | p_x + i p_y | u_v(k) \rangle$$

$$|P_\pm^{vc}(k)|^2 \propto \left(1 \pm \tau \frac{\Delta'}{\sqrt{\Delta'^2 + 4a^2t^2k^2}}\right)^2$$

$$\Delta' = \Delta - \tau s \lambda$$

Zeng, *et al*, Nature Nano **7**, 490 (2012)

T. Cao, *et al* Nature Commuin. DoI: 10.1038/ncomms1882 (2012)

Charged excitons (MoSe2: Trion)

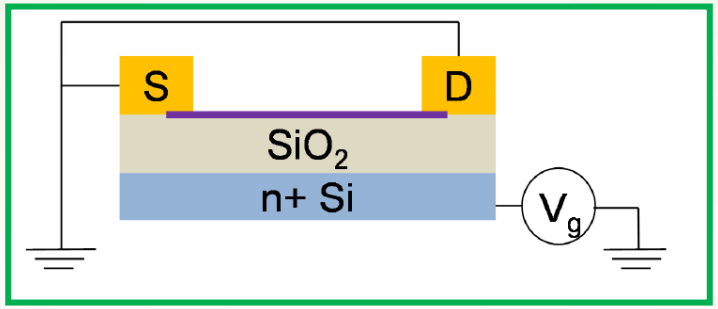

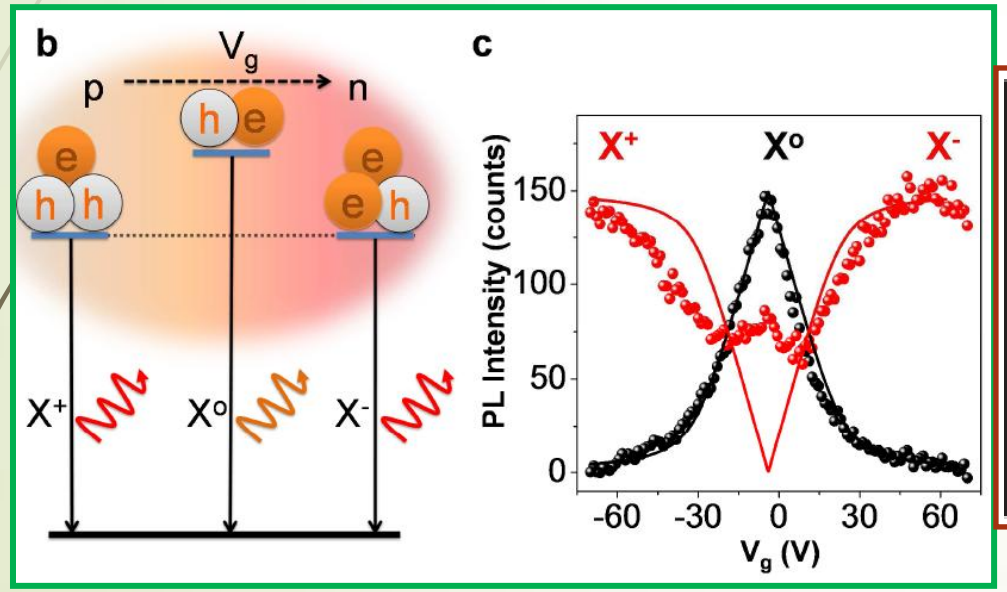

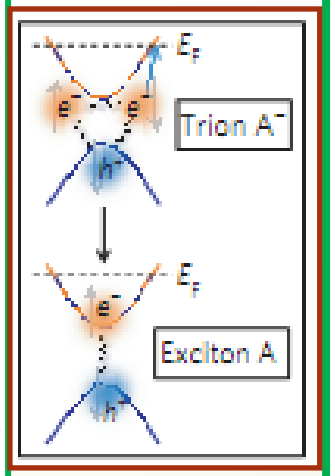

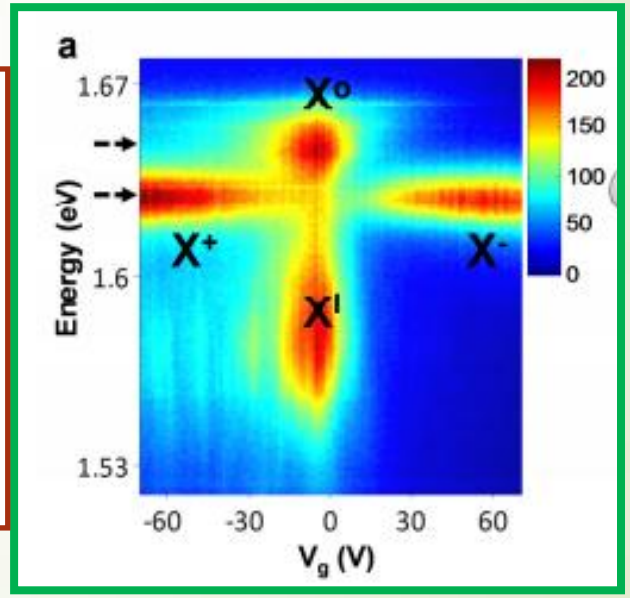

K. F. Mak *et al*, Nature Materials **12**, 207 (2013)

J. S. Ross *et al*, Nature Communi. **4**, 1474(2013)

TMDCs: MoS2 crystal

Nanoelectronic properties

Scattering mechanisms

- Charged impurities(Coulomb scattering)
- Neutral defects (short range scattering)
- Surface interface phonon scattering
- Ripples and roughness scattering
- Acoustic and optical phonons scattering

2D Semiconductor

$$\mu_{charged} \approx \left(m_e^*\right)^{-1/2} T^{3/2}$$

$$\mu_{optical} \approx \left(m_e^*\right)^{-5/2} T^{-1} \left[e^{\frac{\omega_{op}}{T}} - 1 \right]$$

$$\mu_{acoustic} \approx \left(m_e^*\right)^{-5/2} T^{-3/2}$$

$$\mu(T) \approx \begin{cases} T \prec\prec 1 & 10^4 & (1978) \\ T \prec\prec 1 & 3\times 10^6 & (2000) \\ T = 300 & 1000 & (2000) \end{cases}$$

Typical electron mobility for Si at room temperature (300 K) is 1400 $cm^2/(V\cdot s)$ and the hole mobility is around 450 $cm^2/(V\cdot s)$.

Phonons, Raman Spectroscopy

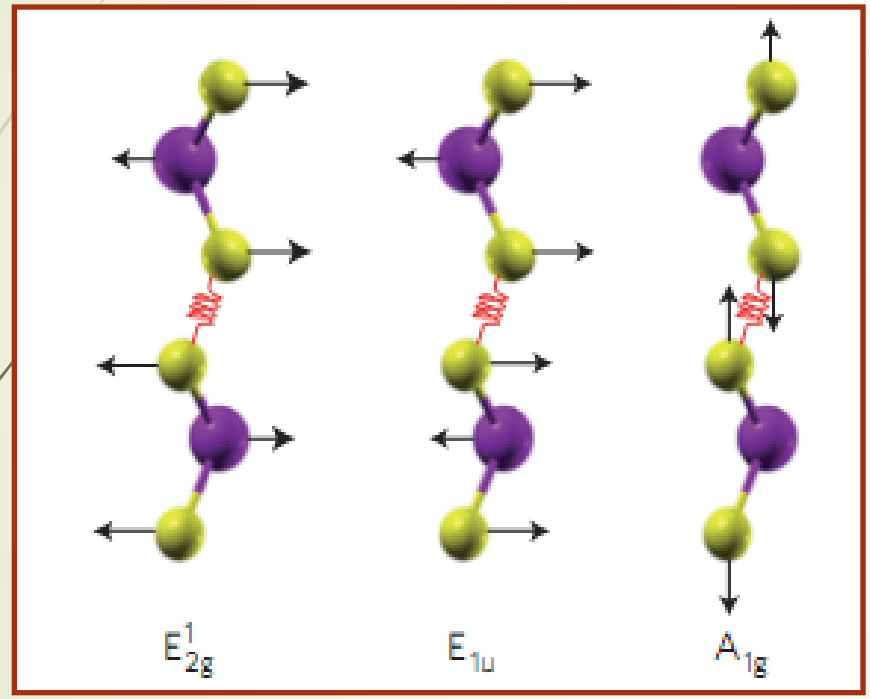

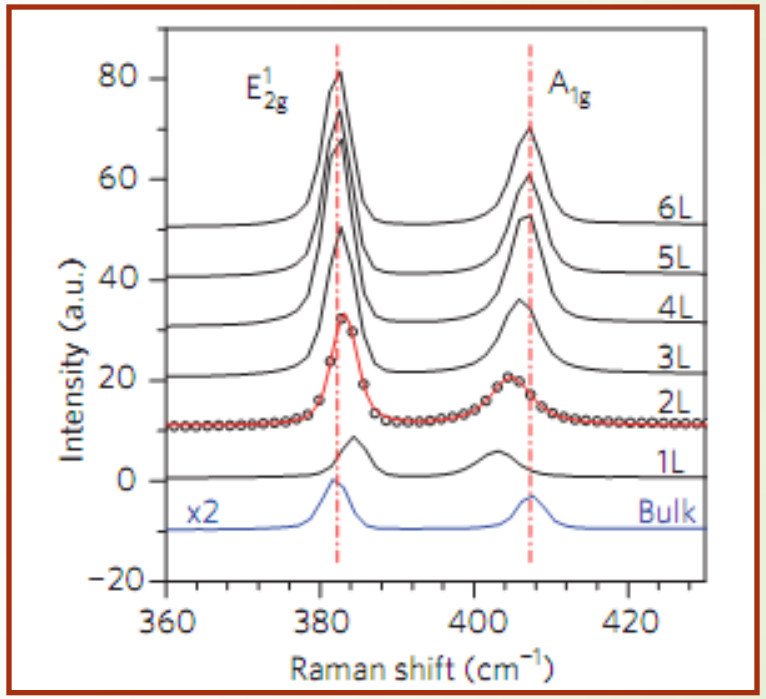

Molina-Sanchez, Wirtz, Phys. Rev. B **84**, 155413 (2011)
Lee *et al*., ACS Nano, **4**, 2695 (2010)

Mobility: evidence

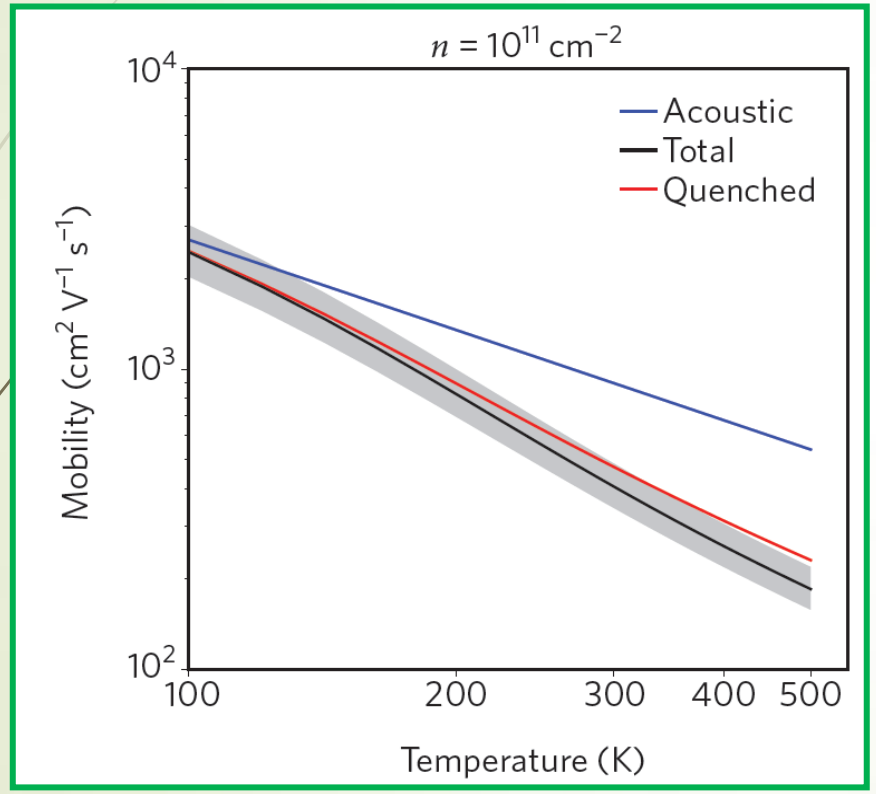

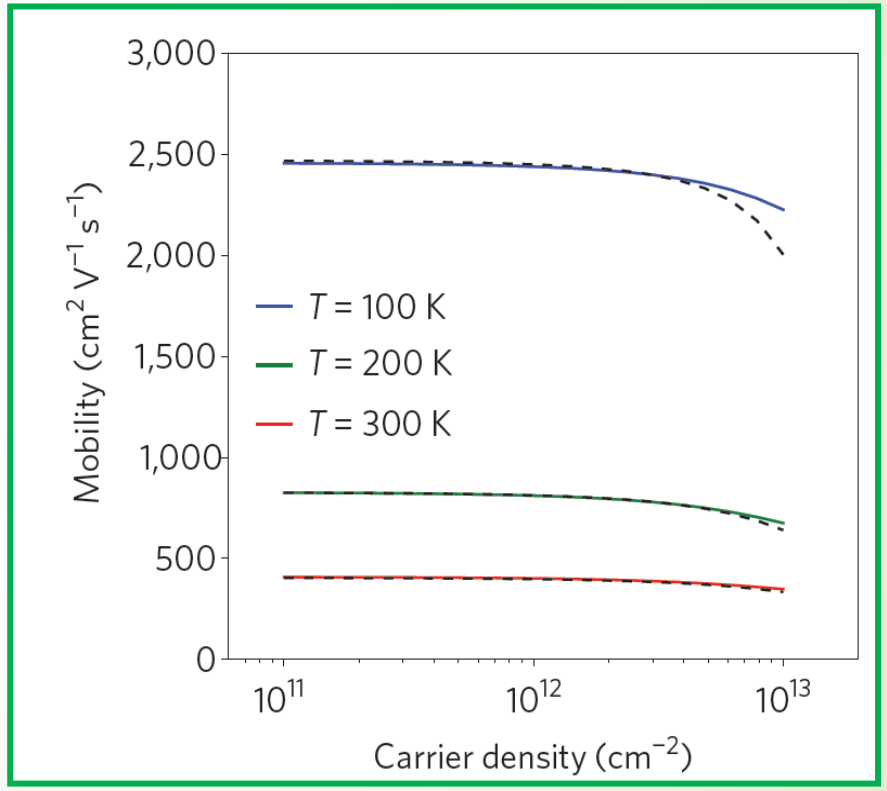

Kaasbjerg, *et al.*, *Phy. Rev. B* **85**,115317 (2012)

MoS2 Transistor

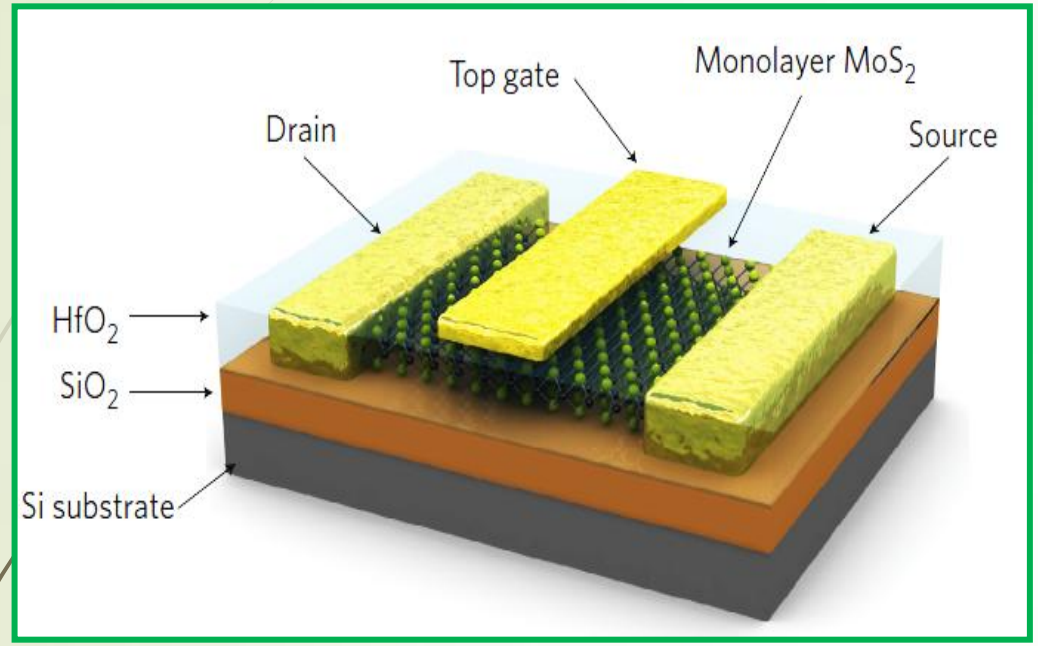

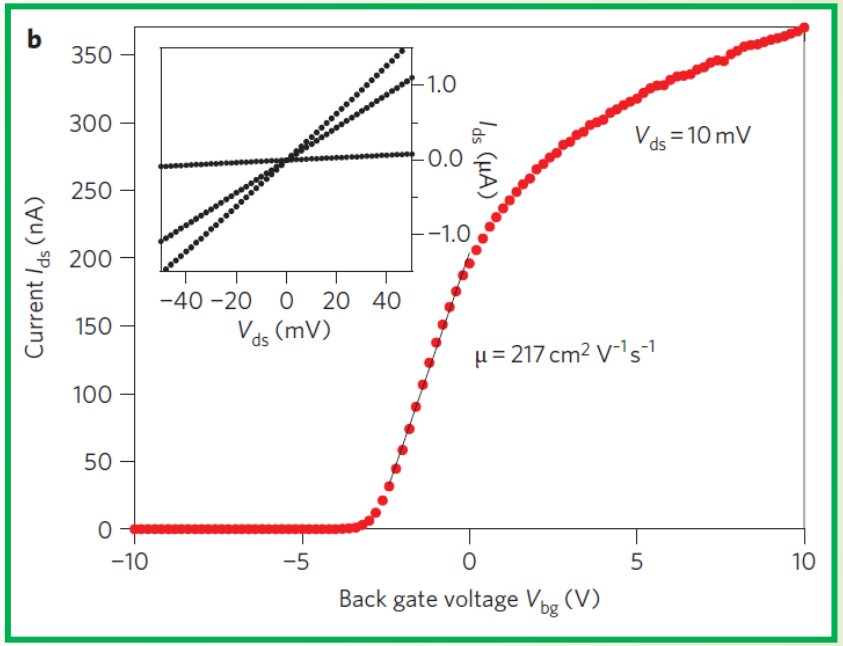

Beritnell, *et al.*, Science **335**, 947 (2012)

Yoon *et al.*, Nano Lett. **11**, 3768 (2011)

Radisavljevic, Nature Nano, **6,** 147 (2011)

Superconductivity

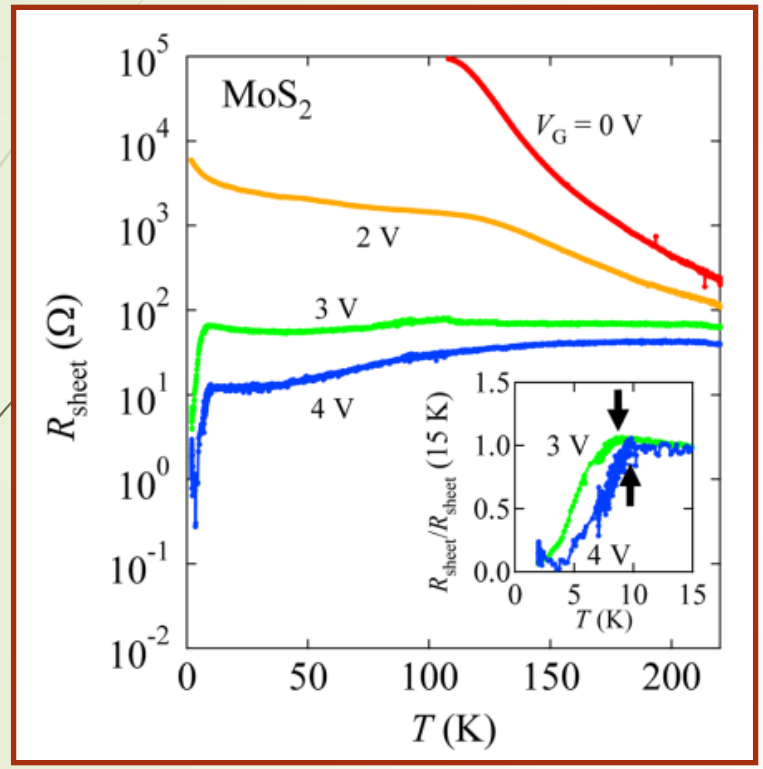

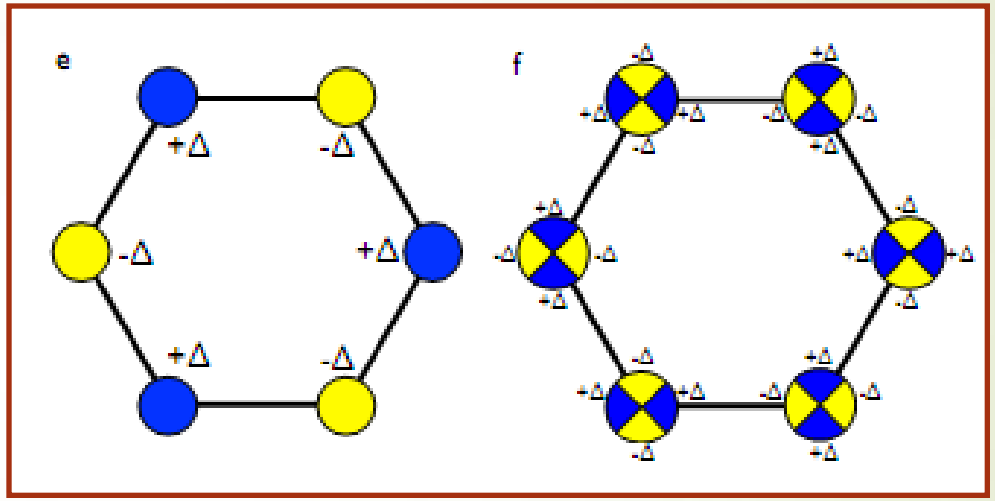

Ztaniguchi *et al.*, Appl. Phys. Lett. **101**, 042603 (2012)

Roldan, Cappelluti and Guinea, arXiv: 1301.4836

Thanks for your attention